

Monte Carlo Analysis of Satellite Beam Pointing Errors

Robert O. Hughes

General Electric Company, Philadelphia, Pennsylvania 19101

Imperfections in attitude control components and control algorithms of communications satellites result in spacecraft pointing errors and give rise to a random variation of the radiated power delivered to the ground. Monte Carlo techniques are applied to this statistical problem to obtain design and margin information. A probabilistic method of specifying required power levels is presented.

Introduction

AN important measure of performance for communications satellites is the amount of effective isotropic radiated power (EIRP) that can be delivered to specific Earth locations. In many cases, radio frequency (RF) beam patterns are shaped to increase EIRP for particular geographic areas. A specific example of such a communications satellite with a specially shaped antenna beam pattern is a geosynchronous, three-axis, stabilized Direct Broadcast Satellite (DBS)^{1,2} that transmits to the Eastern Service Area (ESA) of the United States. This satellite typically would be stationed at 115° west longitude and have a view of the ESA and Central Service Area (CSA) as shown in Fig. 1. To cover the ESA most effectively, the satellite's transmit antenna should be pointed in a direction offset from the nadir-pointing yaw axis of the satellite. This pointing direction is controlled by antenna mounting angles α and β , and the offset pointing of the beam center from the satellite is shown in Fig. 2.

Spacecraft Attitude Control Errors

Three-axis stabilization of the communication satellites considered in this study is achieved using reaction wheels, control algorithms residing in an onboard computer, and sensors (an Earth sensor for pitch/roll and a Sun sensor for yaw). These actuators, algorithms, and sensors are not error free, and pointing errors will exist. Because the algorithm design of the attitude control subsystem and the actuation technique is continuous or vernier, these pointing errors can be approximated by zero-mean Gaussian distributions. The 3σ values of these distributions can be approximated by the maximum expected roll, pitch, and yaw pointing errors. If thrusters were used, then the actuation technique would be of the on/off (or bang-bang) type, and a uniform distribution would be a more appropriate model³ to characterize the pointing errors.

Because of the small angular offsets of the antenna, spacecraft roll and pitch errors affect ground power variation in direct north/south and east/west directions, respectively. That is, a roll error of 1 deg will result in a shift of the antenna pattern in the north/south direction of about 1 deg. However, yaw errors will cause the offset beam center to move in an arc

S as depicted in Figs. 2 and 3. This motion, in turn, results in ground power variations in both the north/south and east/west directions as shown in the representation of an idealized flat Earth model of Fig. 3.

Beam Center Characteristics Using Monte Carlo Techniques

Let θ , ϕ , and ψ be the normally distributed independent random variables that represent the roll, pitch, and yaw spacecraft attitude errors and let σ_R , σ_P , and σ_Y be the standard deviations of these random variables. For the idealized Earth without curvature, the probabilistic behavior of the beam center in the east/west and north/south directions can be represented by the two new random variables:

$$X = \phi + R \sin(\gamma)\psi \quad (\text{east/west}) \quad (1)$$

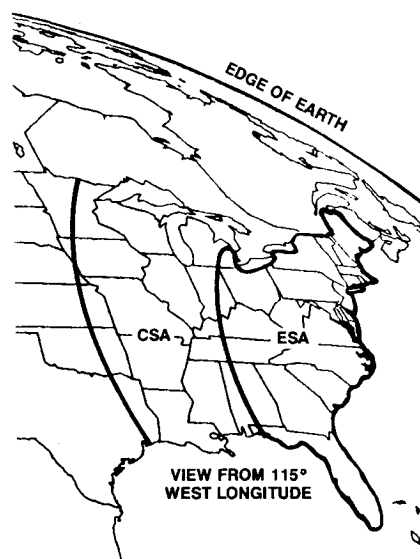
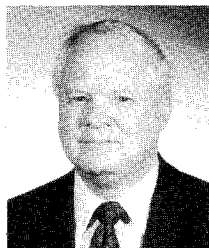


Fig. 1 Satellite view of two service areas.



Dr. Robert O. Hughes was born in Grand Tower, Illinois, and was graduated from the U.S. Naval Academy, Annapolis, Maryland, in 1964. He received his M.S. and Ph.D. degrees in Mechanical Engineering (Control Systems) from the University of Illinois, Urbana-Champaign, Illinois, in 1972 and 1974, respectively. He was a Member of the Technical Staff at the Jet Propulsion Laboratory, Pasadena, California, where he analyzed and designed flight control systems for various projects, including the Viking and Voyager missions. Currently, Dr. Hughes is with the Astro-Space Division of the General Electric Company, Philadelphia, Pennsylvania, and works in the area of satellite attitude control systems. His interests include precision pointing systems, control and structural interaction of large flexible spacecraft, control of solar/wind power generation systems, and applied statistical methods.

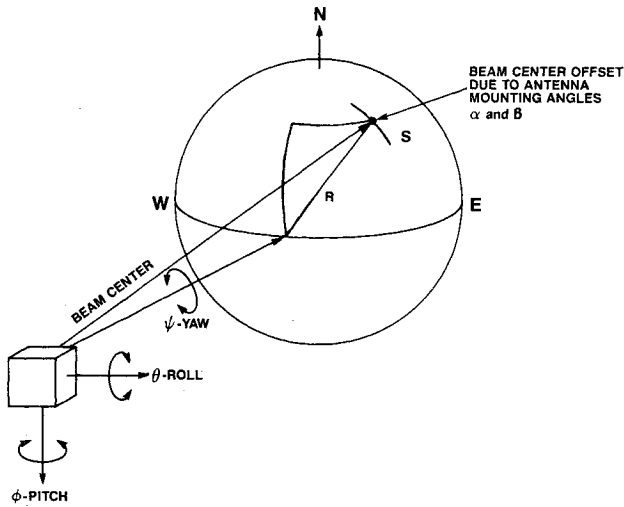


Fig. 2 Spacecraft axes and beam center offset.

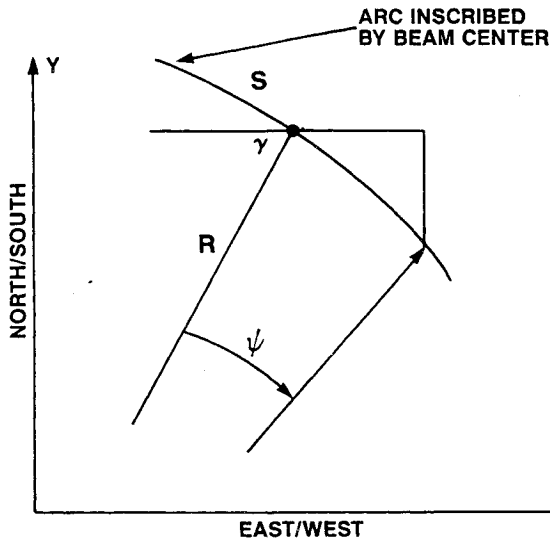


Fig. 3 Effect of a yaw spacecraft error on motion of beam center.

$$Y = \theta - R \cos(\gamma)\psi \quad (\text{north/south}) \quad (2)$$

where

$$R = \sqrt{\alpha^2 + \beta^2} \quad (3)$$

$$\gamma = \arctan(\beta/\alpha) \quad (4)$$

and α and β are the mounting offset angles of the antenna.

Equations (1) and (2) can be simplified further to

$$X = \phi + \beta\psi \quad (5)$$

$$Y = \theta - \alpha\psi \quad (6)$$

The random behavior of the beam center pointing as given by Eqs. (5) and (6) represents complicated statistics, and Monte Carlo techniques⁴ aid in problem analysis and solution. Monte Carlo is a generic term for a wide range of computational techniques that use random trials to analyze statistical problems. For this beam pointing problem, the Monte Carlo method is applied as follows:

- 1) Generate N sequences of the three normally distributed random variables θ , ϕ , and ψ .
- 2) Generate N pairs of (x, y) points in accordance with Eqs. (5) and (6).

3) Increment an individual counter should an (x, y) pair fall within its appropriate "bin" of a two-dimensional grid system.

After N trials, each bin contains a count of successful trials. If each count is divided by N , then the resulting value represents the probability of that particular (x, y) pointing error occurring. All of the probability values together represent an approximation to a joint probability density function,⁵ $f(x, y)$, of the random variables X and Y . Figure 4 shows this density function for a typical spacecraft parameter set of

$$\alpha = 0.075 \text{ rad (about pitch)}$$

$$\beta = 0.102 \text{ rad (about roll)}$$

$$3\sigma_R = 0.15 \text{ deg} \quad (7)$$

$$3\sigma_P = 0.15 \text{ deg}$$

$$3\sigma_Y = 1.1 \text{ deg}$$

For a case with $3\sigma_Y = 5 \text{ deg}$, a more pronounced northeast/southwest pattern is produced as shown in Fig. 5. Twenty million random trials (N) are used for both the previous cases. If the yaw errors (σ_Y) were zero (implying a perfect yaw control system) and/or the antenna offsets (α and β) were zero, then the joint density function $f(x, y)$ of the random

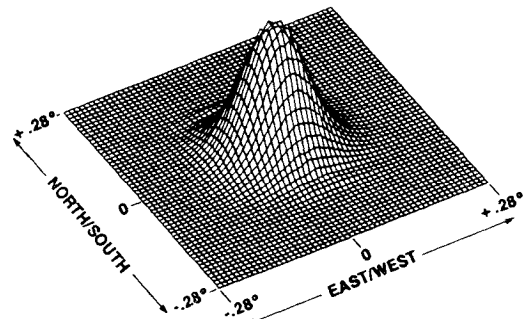


Fig. 4 Pointing error density function for nominal yaw errors.

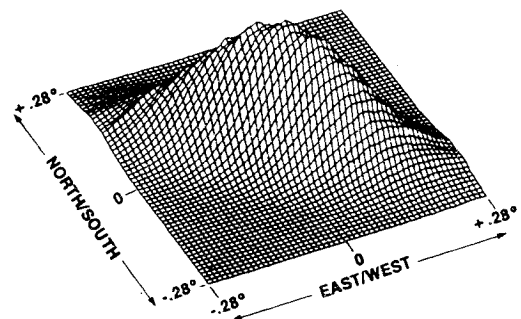


Fig. 5 Pointing error density function for large yaw errors.

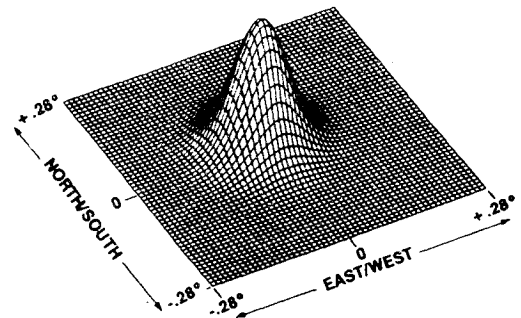


Fig. 6 Pointing error density function for zero yaw error.

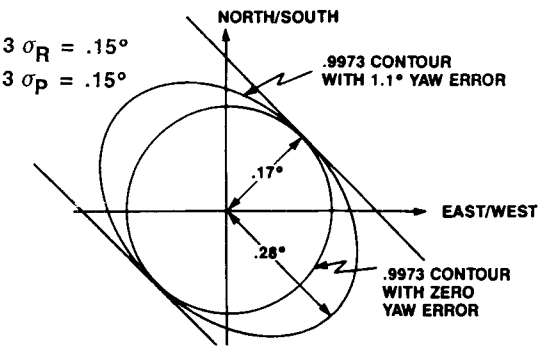


Fig. 7 Probability contours for the nominal density function.

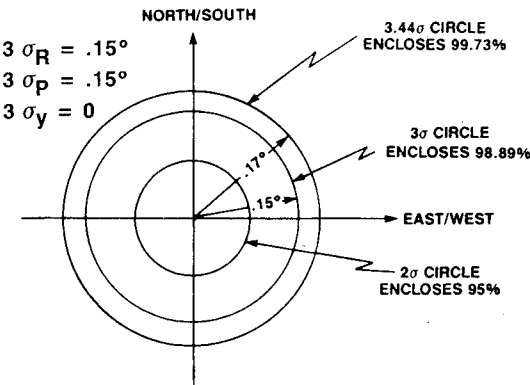


Fig. 8 Probability circles for the bivariate density function.

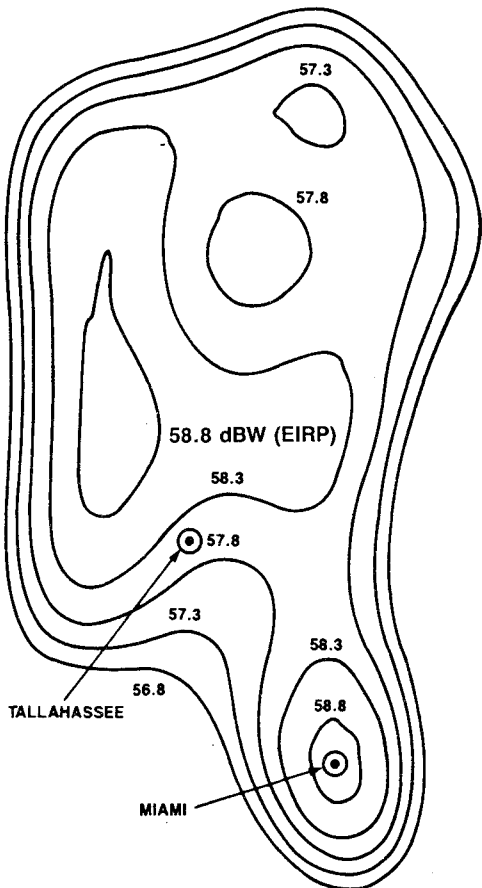


Fig. 9 Shaped beam EIRP pattern for Eastern Service Area.

variables X and Y would be of a standard bivariate normal distribution form and would appear graphically as shown in Fig. 6. This distribution is expressed in closed form⁵ as

$$f(x,y) = \frac{1}{2\pi\sigma_R\sigma_P} \exp \left[-\frac{1}{2} \left(\frac{x^2}{\sigma_R^2} + \frac{y^2}{\sigma_P^2} \right) \right] \tag{8}$$

If bins of nearly equal values of these density functions are connected (thereby forming closed contours), then the total amount of enclosed probability can be calculated. The “skewed ellipse” as shown in Fig. 7 represents the 0.9973 probability contour for the density function of Fig. 4. This ellipse can be compared with its circular companion in Fig. 7 and with the circular probability contours of Fig. 8 for the less complicated, symmetric bivariate density function of Eq. (8). The circles of the symmetric density function enclose probabilities of 0.9973, 0.9889, and 0.95 and are called the 3.44σ , 3σ , and 2σ circles, respectively.

EIRP Specification

A computer-generated shaped-beam EIRP pattern for the ESA is shown in Fig. 9, and more detailed local profiles around the population centers of Miami and Tallahassee are shown in Figs. 10 and 11, respectively. These patterns represent the expected EIRP delivered on the ground without spacecraft motion and are generated using models of the Earth’s curvature. The maximum received power flux density (PFD, in units of dBW/m²) is related to the EIRP values shown in Figs. 9–11 by the equation¹

$$PFD = EIRP - 162.5 \tag{9}$$

Generally,¹ EIRP specifications are defined as a set of “minimum EIRP” values for various geographical locations.

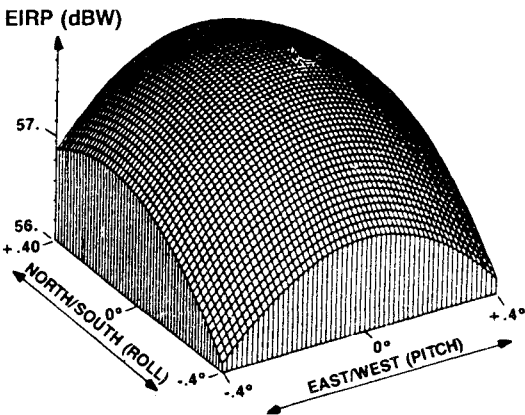


Fig. 10 Local EIRP profile for Miami.

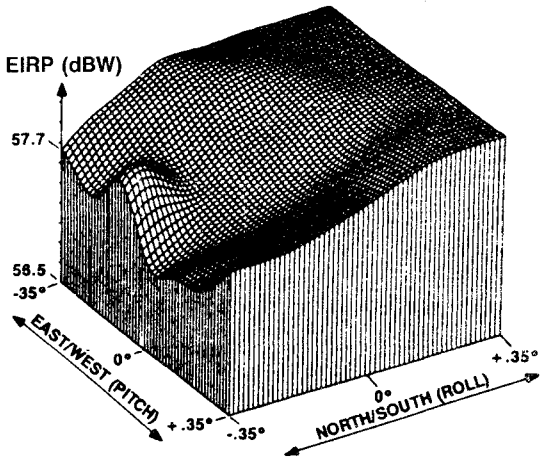


Fig. 11 Local EIRP profile for Tallahassee.

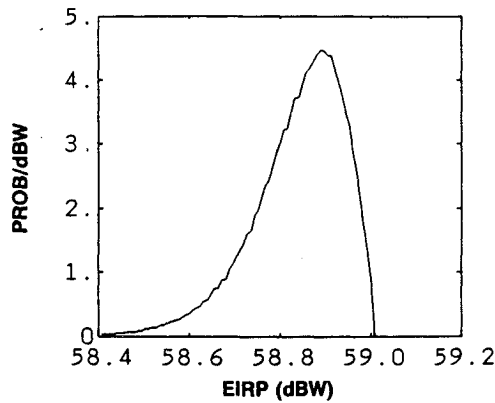


Fig. 12 EIRP probability density for Miami.

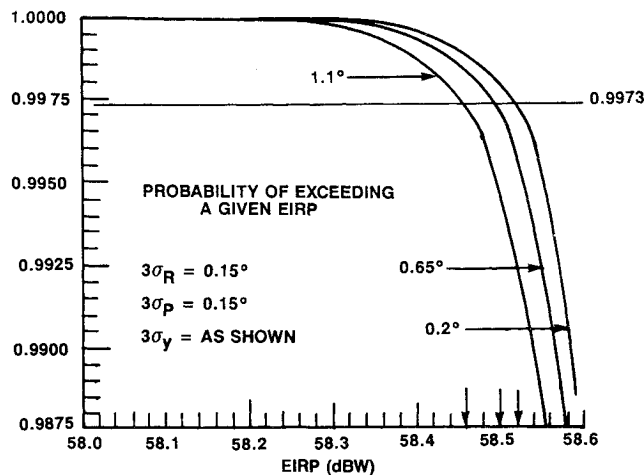


Fig. 13 Cumulative distribution function for Miami.

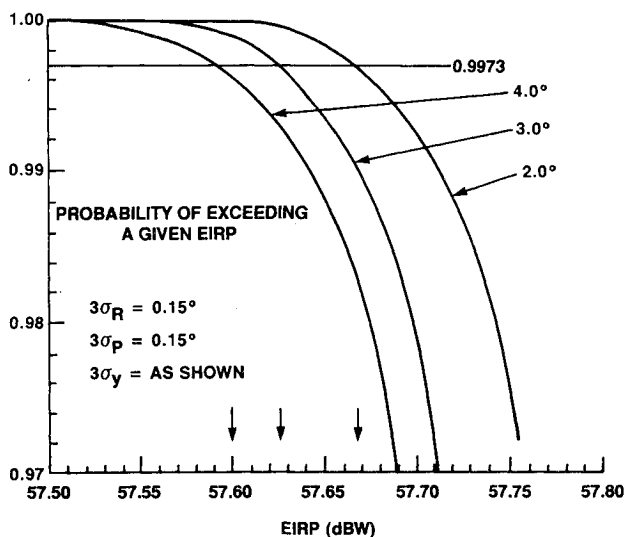


Fig. 14 Cumulative distribution function for Tallahassee.

Statistically, however, zero is the theoretical minimum power level at every location due to spacecraft motion. Thus, for correctness, EIRP specifications should be phrased in probabilistic terms. Such a specification would read as follows: "The probability of exceeding a certain EIRP value at a certain location shall be 0.9973."

The use of the probability value of 0.9973 is somewhat traditional, as it is the area under a standard one-dimensional Gaussian curve between the $\pm 3\sigma$ limits. A probability value

Table 1 Summary of cumulative probability functions

Location	To exceed ^a an EIRP (dBW) of	Requires yaw errors (deg) less than
Miami	58.52	0.2
	58.50	0.65
	58.46	1.1
Tallahassee	57.67	2.0
	57.63	3.0
	57.60	4.0

^aWith a probability of 0.9973.

of 0.9889 could also be used as it represents (see Figs. 6 and 8) the amount of probability (volume) contained within a 3σ circle (cylinder) of the two-dimensional symmetric Gaussian distribution.

In general, it is more difficult and more expensive to meet higher EIRP probability levels because a more accurate spacecraft attitude control system is needed.

EIRP Probability Functions

To determine EIRP specification compliance and/or margins, Monte Carlo techniques, again, are used. Rather than generating the two-dimensional pointing error density functions shown in Figs. 4–6, the randomly generated (x,y) pairs operate on the antenna patterns of Figs. 9–11 to generate a sequence of EIRP values. These values are placed in an appropriate one-dimensional bin system and form a Rayleigh-like density function; an example is shown in Fig. 12 for the nominal parameter set of Eq. (7). This function represents the probability density of a particular value of EIRP occurring at the Miami location. The area under the curve is unity. Note that there is a zero probability density above about 59 dBW, which corresponds to the maximum power level available. Also note that as the density asymptotically approaches zero for decreasing EIRP values, there could be a near-zero power level for a very small, albeit finite period of time. This "tail" is caused by the Gaussian distribution characteristics of the spacecraft control system.

Important design, specification compliance, and margin information are obtained by integrating the EIRP density functions. This integration process generates cumulative distribution functions. Figure 13 shows the cumulative EIRP probability for Miami with small yaw errors, and Fig. 14 shows similar information for Tallahassee with large yaw errors. These figures are summarized in Table 1 for a typical exceedence probability of 0.9973.

Conclusions

Spacecraft motions of a typical geosynchronous communications satellite cause EIRP variations on the ground. Because of geometrical constraints, the yaw attitude motion for a satellite with an offset antenna causes the EIRP pattern to change in a diagonal fashion, and the probability density function of the pointing error is "stretched" in this direction. The use of Monte Carlo techniques simplifies the analysis of resulting pointing errors.

Specifications of minimum EIRPs at certain locations should be phrased in confidence level terms due to the random Gaussian nature of the attitude errors. EIRP cumulative probability functions graphically demonstrate sensitivities and margins. This sensitivity and margin information is necessary to make cost-effective system design tradeoffs.

Acknowledgments

The author wishes to thank N. Alexander and R. Goalwin of the General Electric Company and the anonymous AIAA

reviewer for their constructive comments and insightful reviews of this paper.

References

¹Keane, L. M. (ed.), "A Direct Broadcast Satellite System for the United States," COMSAT Technical Review, Washington, DC, Vol. II, No. 2, 1981.

²Benet, C., Furia, T., Schmidt, G., and Tracy, T., "The Attitude Determination and Control Subsystem of the STC (Satellite Television Corporation) Direct Broadcast Satellite," International Federation of

Automatic Control, Automatic Control in Space, Toulouse, France, 1985.

³Hughes, R. O., "Efficiency Degradation Due to Tracking Errors for Point Focusing Solar Collectors," American Society of Mechanical Engineers, Winter Annual Meeting, San Francisco, CA, Paper 78-WA/Vol-4, Dec. 1978.

⁴Meyer, S., *Data Analysis for Scientists and Engineers*, Wiley, New York, 1975.

⁵Papoulis, A., *Probability, Random Variables, and Stochastic Processes*, 2nd ed., McGraw-Hill, New York, 1984.

*Recommended Reading from the AIAA
Progress in Astronautics and Aeronautics Series . . .* 

Dynamics of Explosions and Dynamics of Reactive Systems, I and II

J. R. Bowen, J. C. Leyer, and R. I. Soloukhin, editors

Companion volumes, *Dynamics of Explosions* and *Dynamics of Reactive Systems, I and II*, cover new findings in the gasdynamics of flows associated with exothermic processing—the essential feature of detonation waves—and other, associated phenomena.

Dynamics of Explosions (volume 106) primarily concerns the interrelationship between the rate processes of energy deposition in a compressible medium and the concurrent nonsteady flow as it typically occurs in explosion phenomena. *Dynamics of Reactive Systems* (Volume 105, parts I and II) spans a broader area, encompassing the processes coupling the dynamics of fluid flow and molecular transformations in reactive media, occurring in any combustion system. The two volumes, in addition to embracing the usual topics of explosions, detonations, shock phenomena, and reactive flow, treat gasdynamic aspects of nonsteady flow in combustion, and the effects of turbulence and diagnostic techniques used to study combustion phenomena.

Dynamics of Explosions
1986 664 pp. illus., Hardback
ISBN 0-930403-15-0
AIAA Members \$54.95
Nonmembers \$92.95
Order Number V-106

Dynamics of Reactive Systems I and II
1986 900 pp. (2 vols.), illus. Hardback
ISBN 0-930403-14-2
AIAA Members \$86.95
Nonmembers \$135.00
Order Number V-105

TO ORDER: Write, Phone, or FAX: American Institute of Aeronautics and Astronautics c/o Publications Customer Service, 9 Jay Gould Ct., P.O. Box 753, Waldorf, MD 20604 Phone: 301/645-5643 or 1-800/682-AIAA, Dept. 415 ■ FAX: 301/843-0159

Sales Tax: CA residents, 8.25%; DC, 6%. For shipping and handling add \$4.75 for 1-4 books (call for rates for higher quantities). Orders under \$50.00 must be prepaid. Foreign orders must be prepaid. Please allow 4 weeks for delivery. Prices are subject to change without notice. Returns will be accepted within 15 days.